IL NUOVO CIMENTO **46 C** (2023) 107
DOI 10.1393/ncc/i2023-23107-9

COMMUNICATIONS: SIF Congress 2022

Magnetic properties of thick synthetic antiferromagnets with different ferromagnetic layers

D. GIRARDI, D. PETTI and E. ALBISETTI
Dipartimento di Fisica, Politecnico di Milano - Milano, Italy

received 14 February 2023

Summary. — Synthetic antiferromagnets (SAF) are versatile magnetic structures consisting of two ferromagnetic thin films with antiparallel magnetization, separated by a thin non-magnetic spacer. They are used in modern spintronics as building blocks of spintronic devices for data storage applications, computing, and as magnetic-field sensors. More recently, they have been proposed as media for efficient skyrmions and spin-waves propagation, and for spin-torque oscillators. Tailoring their properties is therefore of fundamental importance for the development of novel nanomaterials. In this work, the magnetic properties of different types of SAFs are investigated via vibrating sample magnetometry, by changing the thickness of the layers. Importantly, while a decrease of the saturation and interlayer exchange coupling field for thicker systems is present, the desired antiferromagnetic coupling at remanence is still robust. These results suggest that by modulating the thickness of the layers, it is possible to finely engineer the SAF magnetic properties even in tens of nm-thick SAFs, enabling a new degree of freedom in the design and development of novel magnetic nanodevices.

1. – Introduction

Synthetic antiferromagnets (SAFs) are magnetic structures characterized by ferromagnetic (FM) layers antiparallelly coupled at remanence through the presence of a non-magnetic spacer via interlayer exchange coupling (IEC) [1, 2]. They are classified as compensated SAFs, if the structure has zero net magnetization, or uncompensated SAFs, with a small but non-zero net magnetization arising from the difference in magnetic moments of the layers. A key ingredient often present in SAFs is an additional antiferromagnetic (AF) layer to set an exchange bias (EB) [3] to the structure, which pins at remanence the magnetization of the FM layer in contact with it. Historically speaking, they have been crucial for the development of modern spintronics [4, 5]. They have been used in spin valves [6], hard drives [7], magnetic tunnel junctions [8], magnetic random access memories (MRAM) [9] and magnetic biosensors [10] based on giant (GMR) [11] and tunneling magnetoresistance (TMR) [12]. Recently, they have also been investigated for developing spin-torque oscillators [13], for current-driven domain wall [14] and skyrmion [15] motion, for room-temperature spin superfluidity [16] and for the control of propagating spin waves [17, 18]. In this framework, studying the dependence of their magnetic properties as a function of the layers thicknesses is of fundamental importance. While a lot of research has been focused on studying the oscillatory behavior and the

TABLE I. – *Synthetic antiferromagnetic multilayers composition and name coding.*

Sample name	Multilayer composition (dimensions in nm)
EB22	$Si/SiO_2/Co_{40}Fe_{40}B_{20}(22)/Ru(0.5)/Co_{40}Fe_{40}B_{20}(22)/Ir_{22}Mn_{78}(10)/Ru(2)$
EB45	$Si/SiO_2/Co_{40}Fe_{40}B_{20}(45)/Ru(0.5)/Co_{40}Fe_{40}B_{20}(45)/Ir_{22}Mn_{78}(10)/Ru(2)$
EB70	$Si/SiO_2/Co_{40}Fe_{40}B_{20}(70)/Ru(0.5)/Co_{40}Fe_{40}B_{20}(70)/Ir_{22}Mn_{78}(10)/Ru(2)$
EB100	$Si/SiO_2/Co_{40}Fe_{40}B_{20}(100)/Ru(0.5)/Co_{40}Fe_{40}B_{20}(100)/Ir_{22}Mn_{78}(10)/Ru(2)$
C45	$Si/SiO_2/Co_{40}Fe_{40}B_{20}(45)/Ru(0.5)/Co_{40}Fe_{40}B_{20}(45)/Ru(2)$
C70	$Si/SiO_2/Co_{40}Fe_{40}B_{20}(70)/Ru(0.5)/Co_{40}Fe_{40}B_{20}(70)/Ru(2)$
C100	$Si/SiO_2/Co_{40}Fe_{40}B_{20}(100)/Ru(0.5)/Co_{40}Fe_{40}B_{20}(100)/Ru(2)$
NC	$Si/SiO_2/Co_{40}Fe_{40}B_{20}(50)/Ru(0.5)/Ni_{80}Fe_{20}(40)/Ru(2)$

strength of the IEC as a function of the interlayer thickness for SAFs few tens of nm thick [4, 19], a clear picture of their behavior as a function of the FM layers thickness up to hundreds of nm is still missing. Here, we systematically study via vibrating sample magnetometry the magnetic properties of different compensated and non-compensated thick SAFs, both with and without EB, by varying the FM layers thickness.

2. – Experimental details

Three types of SAF structures with thickness from 45 to 200 nm were developed: an EB compensated SAF (fig. 1(a)), a compensated SAF without EB (fig. 1(b)) and an uncompensated SAF without EB (fig. 1(c)). Their composition and name coding is reported in table I. All samples were grown on Si/SiO_2 substrates by magnetron sputtering (AJA ATC Orion 8 system) in RF and DC mode with a pressure below 1×10^{-8} Torr. The EB SAFs were grown with an in-plane applied magnetic field during the deposition process, to set the direction of the magnetocrystalline anisotropy and of the EB, while no in-plane field was present during the growth of the other SAF samples. The hysteresis cycles were measured via a vibrating sample magnetometer (Microsense, LLC. Easy VSM) after deposition. Additionally, for the EB SAFs, the hysteresis loops were analyzed after a field cooling (FC) procedure, performed at 250 °C for 5 min in an in-plane magnetic film of 4 kOe oriented in the same direction as the one applied during the deposition process, to fully set the direction of the EB along the easy axis (EA).

3. – Results and discussion

Figure 1(d) reports the hysteresis cycle of sample EB45 along the EA after deposition and after the FC. The orange and purple arrows represent the direction of the magnetization **M** for the top and bottom FM layers, respectively. For strong negative external

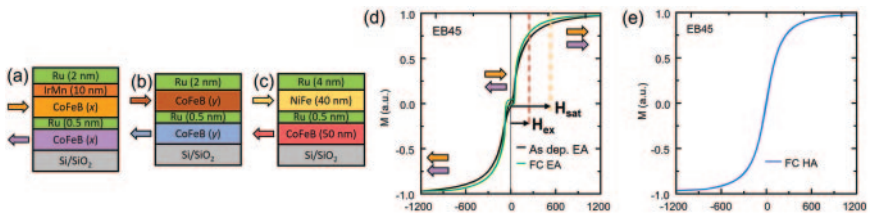

Fig. 1. – (a) EB compensated SAF, (b) compensated SAF without EB and (c) non-compensated SAF without EB; (d) hysteresis loop of EB45 as deposited and after FC, measured along the EA and (e) after the FC, measured along the HA.

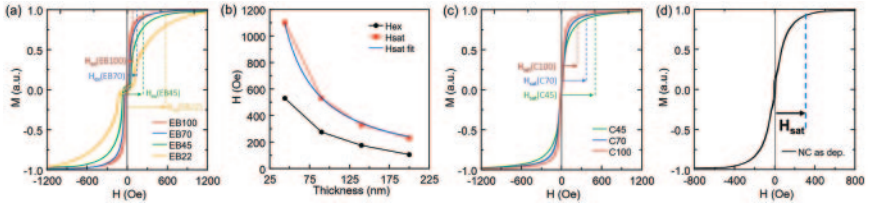

Fig. 2. – (a) Hysteresis loops of the EB SAFs after FC along the EA and identification of $\mathbf{H}_{\rm ex}$; (b) Variation of $\mathbf{H}_{\rm ex}$ and $\mathbf{H}_{\rm sat}$ with multilayer thickness; (c), (d): hysteresis loops of the SAFs without EB (c) and of the non-compensated SAF (d) as deposited and identification of $\mathbf{H}_{\rm sat}$.

fields, $\mathbf{M}$ is saturated along the negative direction, and the magnetic layers are parallelly coupled. Decreasing the field, $\mathbf{M}$ tilts antiparallelly due to the IEC. This behavior is manifested by the plateau at low fields for the EA direction. Finally, by applying a large positive magnetic field, $\mathbf{M}$ is forced along the positive direction. It is possible to observe that after the FC the plateau is better defined with respect to the as-deposited measurement (curve as-deposited EA), since the FC procedure drastically improves the unidirectional anisotropy set via EB. However, it is worth noticing that a small loop in the $\mathbf{H} = 0$ region is still present, due to a slight non-compensation of the two FM layers. This effect can be ascribed to small differences in their deposition conditions and to their surface roughness, leading to the additional Néel coupling term [20]. In fig. 1(d), the saturation field $\mathbf{H}_{\rm sat}$ and the IEC field $\mathbf{H}_{\rm ex}$ are also reported. $\mathbf{H}_{\rm ex}$ is calculated as the point between the plateau and $\mathbf{H}_{\rm sat}$. Importantly, $\mathbf{H}_{\rm sat}$ can be related to the intensity of the IEC strength by $J = -\mu_0 \mathbf{H}_{sat} M_s t/2$ (with t as the thickness of the layers, J the IEC constant and $\rm M_s$ the saturation magnetization) [5]. In addition to this, fig. 1(e) shows the hysteresis cycle of the sample EB45 along the HA after the FC. In this case, since the loop is measured in the direction perpendicular to the unidirectional anisotropy set via EB, corresponding to the energetically less favourable orientation for the magnetization, no hysteresis at remanence is observed. Figure 2(a) shows the hysteresis cycles and the corresponding values of $\mathbf{H}_{\rm ex}$ of all EB SAF samples along the EA after FC. In all the samples, the loops feature the low-field plateau typical of AF coupling between the FM layers. Noticeably, despite the decrease in the intensity of $\mathbf{H}_{\rm ex}$ and $\mathbf{H}_{\rm sat}$ when increasing the thickness of the FM layer, even for thick SAFs the IEC is large enough to allow for a sufficiently robust AF coupling, as can be seen by the presence of the plateau at low fields for all loops. A quantitative study is reported in fig. 2(b), where the variation of the intensity of $\mathbf{H}_{\rm sat}$ and $\mathbf{H}_{\rm ex}$ with respect to the thickness of the whole structure is shown. As expected, the values of $\mathbf{H}_{\rm sat}$ decrease as a function of $1/t$, as can be fitted by the function $\mathbf{H}_{sat} = -2J/\mu_0 M_s t$. The same dependency with t can also be appreciated for $\mathbf{H}_{\rm ex}$. From it, we can calculate $J \sim -1.48 \pm 0.03$ mJ/m^2, similar to other reported values for systems based on CoFeB/Ru/CoFeB layers [17]. On the other hand, for the SAF samples without the AF layer, since no EB is present, the FC process was not performed. The hysteresis cycles reported in fig. 2(c) were measured only after deposition, and because no in-plane field was applied during the growth process, no defined anisotropy direction is present. Nevertheless, the correct AF coupling of the layers is proven by the lack of hysteresis and the remanence, *i.e.*, $\mathbf{M} = 0$ at $\mathbf{H} = 0$ and by the presence of the typical inflection point for the curve. Also in this case, $\mathbf{H}_{\rm sat}$ decreases for the thicker SAFs. The extracted value of the IEC constant for these samples is $J \sim -1.42 \pm 0.02$ mJ/m^2, comparable to the EB compensated SAF based on the same structure. Finally, the loop of the non-compensated SAF without EB is reported in fig. 2(d). Importantly, being based on

CoFeB and NiFe layers, the difference in M_s of the layers gives rise to a non-compensation of **M** in the antiparallel configuration, resulting in the presence of a visible loop at low fields, even with no anisotropy set during deposition. In this case, the IEC constant can be estimated as $J \sim -0.8$ mJ/m^2, lower with respect to the values of $J \sim -1.48$ mJ/m^2 and $J \sim -1.42$ mJ/m^2 for the EB compensated SAF and compensated SAF without EB, respectively.

4. – Conclusions

In this work, the dependence of the magnetic properties of different compensated and non-compensated thick SAFs is investigated via VSM, with total thickness ranging from 45 nm to 200 nm. Noteworthy, while a decrease in $\mathbf{H}_{sat}$ and $\mathbf{H}_{ex}$ for thicker samples is observed, the IEC strength, evaluated for all different SAFs as the IEC constant, is enough to grant the antiferromagnetic coupling for all samples. On the other hand, we show that by a suitable choice of thickness of the FM layers, the values of $\mathbf{H}_{sat}$ and $\mathbf{H}_{ex}$ can be modulated. These results suggest that SAFs up to hundreds of nm thick can be successfully realized via magnetron sputtering. Furthermore, we show that their hysteresis loop can be finely tuned by controlling the thickness and composition, maintaining a sizeable IEC coupling constant. This makes thick SAF structures a viable route for developing novel magnetic nanodevices for spintronics and magnonics.

* * *

This work was partially performed at PoliFAB, the microtechnology and nanotechnology centre of the Politecnico di Milano. The research leading to these results has received funding from the European Union's Horizon 2020 research and innovation programme under grant agreement number 948225 (project B3YOND). This work has been supported by the FARE programme of the Italian Ministry for University and Research (MIUR) under grant agreement R20FC3PX8R (project NAMASTE). This work has been supported by Fondazione Cariplo and Fondazione CDP, grant No. 2022-1881.

REFERENCES

[1] Grünberg P. *et al.*, *J. Appl. Phys.*, **61** (1987) 3750.
[2] Unguris J. *et al.*, *Phys. Rev. Lett.*, **67** (1991) 140.
[3] Nogués J. *et al.*, *J. Magn. & Magn. Mater.*, **192** (1999) 203.
[4] Duine R. A. *et al.*, *Nat. Phys.*, **14** (2018) 217.
[5] Amelichev V. V. *et al.*, *Nanobiotech. Rep.*, **16** (2021) 155.
[6] Dieny B. D. *et al.*, *J. Magn. & Magn. Mater.*, **93** (1991) 101.
[7] Childress J. R. *et al.*, *IEEE Trans. Magn.*, **37** (2001) 1745.
[8] Zaleski A. *et al.*, *J. Phys.: Conf. Ser.*, **200** (2010) 052035.
[9] Parkin S. *et al.*, *Proc. IEEE*, **91** (2003) 661.
[10] Albisetti E. *et al.*, *Sens. Actuat. B: Chem.*, **200** (2014) 39.
[11] Parkin S. S. *et al.*, *Phys. Rev. Lett.*, **64** (1990) 2304.
[12] Miyazaki T. and Tezuka N., *J. Magn. & Magn. Mater.*, **139** (1995) 1.
[13] Monteblanco E. *et al.*, *J. Appl. Phys.*, **121** (2017) 013903.
[14] Parkin Stuart S. P. *et al.*, *Science*, **320** (2008) 190.
[15] Legrand William, *Nat. Mater.*, **19** (2020) 34.
[16] Takei So and Tserkovnyak Yaroslae, *Phys. Rev. Lett.*, **112** (2014) 227201.
[17] Albisetti Edoardo, *Adv. Mater.*, **32** (2020) 2070063.
[18] Wintz Sebastian *et al.*, *Nat. Nanotechnol.*, **11** (2016) 948.
[19] Coehoorn R., *Phys. Rev. B*, **44** (1991) 9331.
[20] Néel Louis, *J. Phys. Radium*, **15** (1954) 225.